

Gamma-Irradiated Bacterial Cellulose as a Three-Dimensional Scaffold for Osteogenic Differentiation of Rat Bone Marrow Stromal Cells

Farah Nurlidar^{1*}, Mime Kobayashi², Ade Lestari Yunus¹, Muhamad Yasin Yunus¹, Tita Puspitasari¹, and Darmawan Darwis¹

¹Center for Research and Technology of Isotopes and Radiation Application, The National Research and Innovation Agency, Jl. Lebak Bulus Raya No. 49, Jakarta Selatan 12440, Indonesia

²Nara Institute of Science and Technology, 8916-5 Takayama, Ikoma, Nara 630-0192, Japan

* **Corresponding author:**

tel: +62-21-7690709

email: farah@batan.go.id

Received: January 3, 2022

Accepted: March 20, 2022

DOI: 10.22146/ijc.71823

Abstract: The effect of gamma-irradiation on bacterial cellulose (BC) was investigated in terms of improving its properties as scaffolds for tissue engineering. BC pellicles were exposed to 25, 50, and 75 kGy gamma-ray irradiation, and X-ray diffraction analyses showed that the crystallinity of the BC decreased as stronger irradiation accelerated BC's degradation. Fourier transform infrared spectroscopy of the irradiated BC revealed the appearance of a new peak at 1724 cm⁻¹, indicating the formation of a new carbonyl group due to the cleavage of glycosidic linkages of the BC. Rat bone marrow stromal cells seeded on the gamma-irradiated BC incubated in an osteogenic medium for 14 days produced calcium, a late marker for osteogenic differentiation, as shown by Alizarin Red S (ARS) staining. Gamma-irradiated BC with higher irradiation doses showed intense ARS staining indicating higher calcium deposition. These findings demonstrate the feasibility of using gamma-irradiated BC as a cytocompatible 3D scaffold for bone tissue regeneration.

Keywords: bacterial cellulose; gamma-irradiation; Alizarin Red S staining; osteogenic differentiation; calcium deposition

■ INTRODUCTION

Hydrogels are promising cross-linked three-dimensional (3D) polymeric networks for tissue engineering because of their hydrophilic structure and ability to encapsulate cells and bioactive molecules [1-4]. In addition, the physical, chemical, and biological properties of the hydrogels can be easily tailored to support cell growth and functions [3].

Bacterial cellulose (BC) has shown promise as a 3D scaffold for stem cell encapsulation based on its high purity, high mechanical properties, and excellent biocompatibility [5-6]. BC has also been shown to be an excellent biomaterial for wound healing [5,7-8]. Despite the fact that native BC has extraordinary inherent properties, to enhance the potential of BC, various methods to improve the physical and chemical properties of native BC have been investigated [9-13]. Modified BC, hyaluronic acid, and gelatin scaffolds showed promising

results when they were used as scaffolds for a human glioblastoma cancer cell line [11]. In addition, modification of BC with the succinyl group has been shown to enhance BC's ability to incorporate bone-like hydroxyapatite [14].

Gamma irradiation has been mainly used to sterilize biomedical devices and pharmaceutical products [15-16]. However, irradiation affects the physicochemical characteristics of the irradiated substances. The degradation of polymers is one of the main negative effects [16]. At the same time, other functional properties may be improved. Criado et al. showed that gamma-irradiation of cellulose nanocrystals (CNCs) caused an increase in antioxidant properties of the materials due to the cleavage of glycosidic linkages in the CNCs [9].

The combination of BC and stem cells has the potential to be used for medical applications, especially for bone tissue regeneration. However, BC has high

crystallinity, limiting the diffusion of nutrients, oxygen, and waste, an essential property as a cell culture scaffold. Gamma-ray irradiation on the BC mainly results in the decomposition of the cellulose [9,17-18]. This process changes the physical and chemical properties of cellulose, such as mechanical properties and porosity. Darwis et al. observed that electron beam irradiation influenced the mechanical properties of dried BC that led to its degradation [19]. Previous studies have demonstrated the effect of high-energy irradiation on the degradation of BC, but few studies have evaluated the potential of gamma-irradiated BC in tissue engineering. In this study, the BC pellicle was gamma-irradiated, and changes in the physical, chemical, and thermal properties of the BC were investigated and discussed. Importantly, the effect of gamma irradiation on the cytotoxicity of the BC and its potential as a 3D scaffold for tissue engineering was also investigated.

■ EXPERIMENTAL SECTION

Materials

Ammonium sulfate, sodium hydroxide, and glacial acetic acid were purchased from Merck GmbH, Germany. Potassium bromide (KBr; FTIR grade) was acquired from Sigma-Aldrich (St. Louis, MO, USA). Water-soluble tetrazolium salt (WST-8) was obtained from Dojindo Molecular Technologies Inc. Kumamoto, Japan. All reagents were used without any additional processing.

Instrumentation

Gamma-ray irradiation was conducted in a gamma cell facility (cobalt-60; Gamma Cell 220 Upgraded, Izotop, Hungaria) at the Center for Research and Technology of Isotopes and Radiation Application (The National Research and Innovation Agency, Indonesia). X-ray diffraction (XRD) analysis was carried out with a RINT-TTR III X-ray diffractometer (Rigaku, Tokyo, Japan). Fourier transform infrared (FTIR) spectra were recorded using a Prestige-21 FTIR spectrometer (Shimadzu, Kyoto, Japan). A DSC-60 differential scanning calorimeter (DSC; Shimadzu, Kyoto, Japan) was used for thermal analysis.

Procedure

Preparation of BC

Bacterial cellulose (BC) was prepared using coconut water as a fermentation medium. Briefly, 1 L of fresh coconut water medium containing 50 g of sucrose (5% w/v) and 5 g of ammonium sulfate (0.5% w/v) was boiled. The pH of the medium was adjusted to pH 4 using glacial acetic acid. The medium was then equilibrated to room temperature prior to use. Ten percent of the pre-culture medium containing *Acetobacter xylinum* was then added into the flask containing the coconut water medium. The mixture was incubated at room temperature under static conditions for 3–4 days. The obtained BC pellicles were then washed with distilled water and immersed in 0.1 M sodium hydroxide at 60 °C for 4 h to remove any residual bacteria. Finally, the BC pellicles were rinsed with distilled water at room temperature to achieve a neutral pH. The pellicles of pure BC were then immersed in distilled water and kept at 4 °C prior to use.

Gamma-irradiation of BC

BC pellicles were placed in the polyethylene plastic bag and then irradiated in a gamma cell facility at a dose rate of 5.5 kGy/h. The irradiation doses were 0, 25, 50, and 75 kGy. After gamma-irradiation, the BC pellicles were extensively washed with distilled water to remove any soluble degradation products and freeze-dried to obtain dried BC.

XRD of gamma-irradiated BC

XRD analysis of the freeze-dried BC was carried out with an X-ray diffractometer in a 2θ range between 10° and 40° with a scanning step of 0.05°. The degree of crystallinity of the BC was evaluated by deconvolution of the XRD diffractogram after a peak-fitting process performed by Fityk 0.9.8 software [20-21]. The degree of crystallinity was calculated as the ratio of the area of crystalline peaks to the total area [20,22].

FTIR analysis of gamma-irradiated BC

FTIR spectra of the freeze-dried BC were recorded in the range of 400–4000 cm^{-1} based on the KBr method

with 45 scans and a resolution of 2 cm⁻¹. All samples were ground with KBr before measurement.

Thermal characteristics of gamma-irradiated BC

DSC was used to study the thermal characteristics of BC before and after gamma-irradiation. All DSC measurements were carried out with a crimped empty pan (aluminum pan, Shimadzu, Tokyo, Japan) as a reference. The reference and crimped pans containing samples were measured at the heating rate of 15 °C/min under a nitrogen atmosphere at a temperature range of 30–500 °C.

Cytotoxicity of gamma-irradiated BC

HeLa cells were cultured in an alpha-minimum essential medium (alpha-MEM; Gibco Invitrogen Corp. Grand Island, NY, USA) containing 10% fetal calf serum (FCS; HyClone, Logan, UT, USA) and cultured in a 25 cm² tissue culture flask (163371; Nalge Nunc International, Roskilde, Denmark) at 37 °C under 5% CO₂. After three days, the attached cells were washed with PBS and treated with an aliquot of 0.02% ethylenediaminetetraacetic acid (EDTA) and 0.25% trypsin. After centrifugation at 1,200 rpm for 5 min, the supernatant was removed, and the cell pellet was suspended in 10% FCS/alphaMEM. The HeLa cell suspension was then prepared at a density of 25,000 cells/mL.

One hundred microliters of cell suspension containing 2,500 cells were cultured in wells of a 96-well plate (Nunc, Denmark) and incubated for 24 h at 37 °C under 5% CO₂. After 24 h, gamma-irradiated BC was added into well-containing cells. The same number of cells without any addition of the BC was used as a 2D control. According to the manufacturer's instructions, the viable cells on days 1 and 2 were quantified using WST-8 reagent. The optical density at 450 nm was measured using a SpectraFluor Plus microplate reader (Tecan, Männedorf, Switzerland). The relative cell viability was calculated, as defined by Eq. (1):

$$\text{Cell viability (\%)} = \frac{(\text{OD}_{450} \text{ sample} - \text{OD}_{450} \text{ medium})}{(\text{OD}_{450} \text{ control} - \text{OD}_{450} \text{ medium})} \times 100\% \quad (1)$$

Encapsulation of rat bone marrow stromal cells on gamma-irradiated BC

Bone marrow cells (BMCs) were harvested from the femora of a six-week-old female Wistar rat. The obtained

rBMSCs were suspended in 20% FCS/alpha-MEM and cultured in an 80 cm² tissue culture flask (153732; Nalge Nunc International) at 37 °C under 5% CO₂ atmosphere. After three days, the attached cells were washed with PBS and treated with an aliquot of 0.02% EDTA and 0.25% trypsin. After centrifugation at 1,200 rpm for 5 min, the supernatant was removed, and the cell pellet was re-suspended in 10% FCS/alpha-MEM. The rBMSC suspension was prepared at a density of 5 × 10⁶ cells/mL. The gamma-irradiated BC scaffolds were put on 24 well-plate. The rBMSC suspension was then seeded on the BC scaffolds at a density of 5 × 10⁴ cells/scaffold and incubated at 37 °C under 5% CO₂. After three hours, 1 mL of medium was added to the dish containing the scaffold. On day 1, the medium was supplemented with an osteogenic supplement of 10 nM dexamethasone, 100 μM L-ascorbic acid-2-phosphate, and 10 mM beta-glycerophosphate, and incubated at 37 °C under 5% CO₂ atmosphere for 14 days. Half of the medium was replaced with a fresh osteogenic medium every two or three days.

The osteogenic differentiation of the rBMSCs in the scaffold was observed using Alizarin Red S (ARS) staining. The BC containing rBMSCs were washed three times with demineralized water and freeze-dried. The dried BC was then incubated in 2% of ARS staining solution for 30 min at room temperature. The BC was then washed four times with demineralized water to remove the excess stain, dried at room temperature, and observed with an optical microscope.

Statistical analysis

All statistical analyses were carried out using the one-way analysis of the variance routine of KaleidaGraph v. 4.5 (Synergy Software, Reading, PA, USA). Tukey's honest significant difference test was used to determine whether or not there were any differences between groups. A value of $p < 0.05$ was accepted as statistically significant. All data were expressed as mean ± standard deviation, with $n = 3$.

RESULTS AND DISCUSSION

XRD Analysis of Gamma-Irradiated BC

XRD analysis was conducted to investigate the influence of gamma-irradiation on the microstructures

of the BC. XRD diffractograms of BC before and after gamma-irradiation showed three main peaks located at $2\theta = 14.4^\circ$, 16.7° , and 22.6° (Fig. 1), which correspond to the $(1\bar{1}0)$, (110) , and (200) plane of cellulose I β , respectively [23-24]. These results are consistent with previous reports of BC production using the static culture method [25].

The degree of crystallinity of the BC was evaluated using the XRD deconvolution method [22]. An example of an XRD diffractogram after a curve fitting process using a Gaussian function is presented in Fig. 2. One amorphous and five crystalline peaks are observed in the XRD deconvolution spectra of BC and gamma-irradiated

BC. Table 1 shows the degree of crystallinity of the gamma-irradiated and native BC. The degree of crystallinity of BC irradiated at 25, 50, and 75 kGy shows a significant decrement compared to native BC ($p < 0.001$). This study revealed that the crystalline area of the BC was disrupted by the gamma irradiation. Similar results have shown that the crystallinity of cellulose was reduced significantly after high-energy radiation [26-27].

FTIR of Gamma-Irradiated BC

FTIR measurement was conducted to observe the influence of gamma-irradiation on the chemical structure

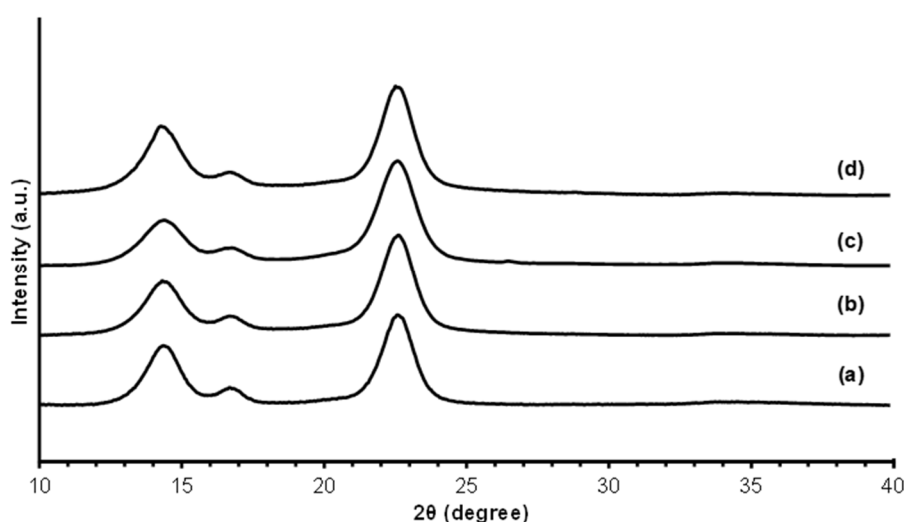


Fig 1. XRD diffraction patterns of native BC (a) and gamma-irradiated BC at 25 (b), 50 (c), and 75 (d) kGy

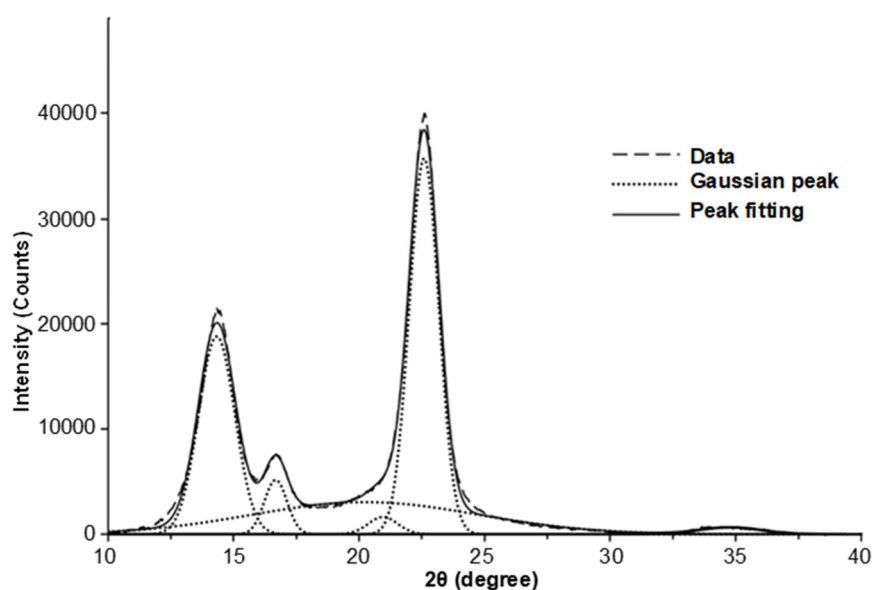


Fig 2. XRD deconvolution peak using a Gaussian function of gamma-irradiated BC 25 kGy with an R^2 value of 0.99766

Table 1. Degree of crystallinity of gamma-irradiated BC ($p < 0.001$)

Irradiation dose (kGy)	Degree of crystallinity (%)
0	82.16 ± 0.73
25	74.21 ± 2.81
50	72.17 ± 0.26
75	64.51 ± 2.65

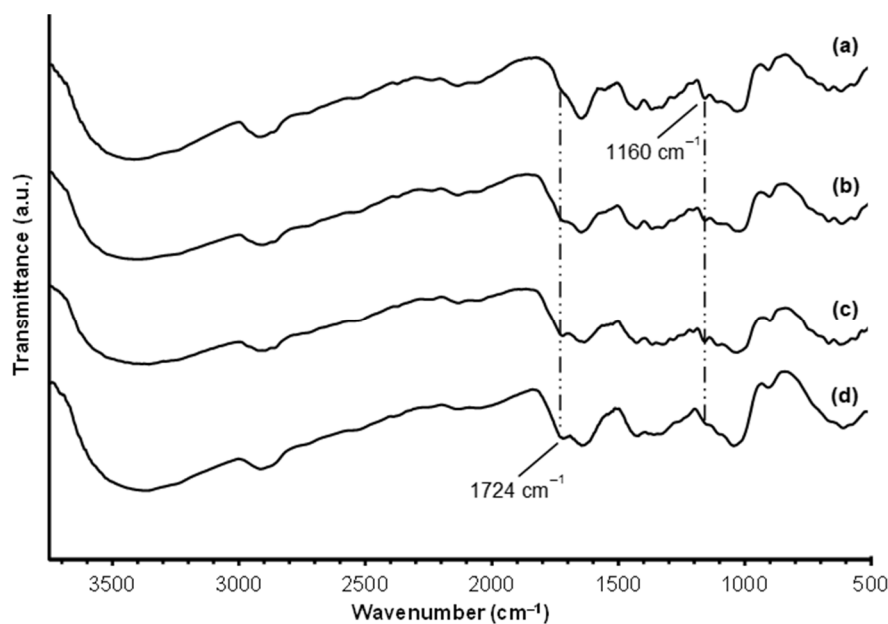
of the BC. Fig. 3 shows the FTIR spectra of BC before and after gamma irradiation. From the spectra, we can see the appearance of a new peak at 1724 cm^{-1} , which correlated to the formation of a new carbonyl group in the gamma-irradiated BC, similar to previous research [9,17-18,27]. It can also be seen from Fig. 3 that the intensity of the peak at 1724 cm^{-1} increased as the irradiation dose increased. In addition, Fig. 3 also shows the disappearance of the peak at 1160 cm^{-1} that correlated to the stretching vibration of the C–O–C glycosidic linkage in the BC structure.

Many authors reported that gamma-irradiation led to cleavage of the glycosidic linkage and the formation of carbonyl groups in the cellulose structure [9,17-18,27]. Bouchard et al. also reported a linear relationship between carbonyl concentration and the irradiation doses [18]. This study confirmed that gamma-irradiation might cause

the breakage of glycosidic linkage and the formation of the carbonyl group in the BC structure.

Thermal Behavior of Gamma Irradiated BC

Thermal properties of the native and gamma-irradiated BC were investigated by DSC, and the results are presented in Fig. 4. The exothermic peak of gamma-irradiated BC at 0, 25, 50, and 75 kGy were 358.57 , 330.12 , 324.50 , and $322.77\text{ }^{\circ}\text{C}$, respectively. These peaks indicate the thermal decomposition of the BC [25,28]. The results showed that the degradation temperature of native BC (0 kGy) is higher than that of the gamma-irradiated BC. The decrease in the degradation temperature of the gamma-irradiated BC could be attributed to the radiation-induced degradation of the polymer chains in the BC. It can also be associated with the cleavage of the glycosidic linkage in the BC structure, as confirmed by the FTIR results. Furthermore, it is well known that the degradation induced by high-energy irradiation may destroy the structure of BC. Thus, the irradiation may have enhanced the amorphous peak in the BC structure, as indicated by the XRD results. These results implicated that irradiation doses have a significant contribution to the physical and chemical properties of the BC.

**Fig 3.** FTIR spectra of gamma-irradiated BC at 0 (a), 25 (b), 50 (c), and 75 (d) kGy

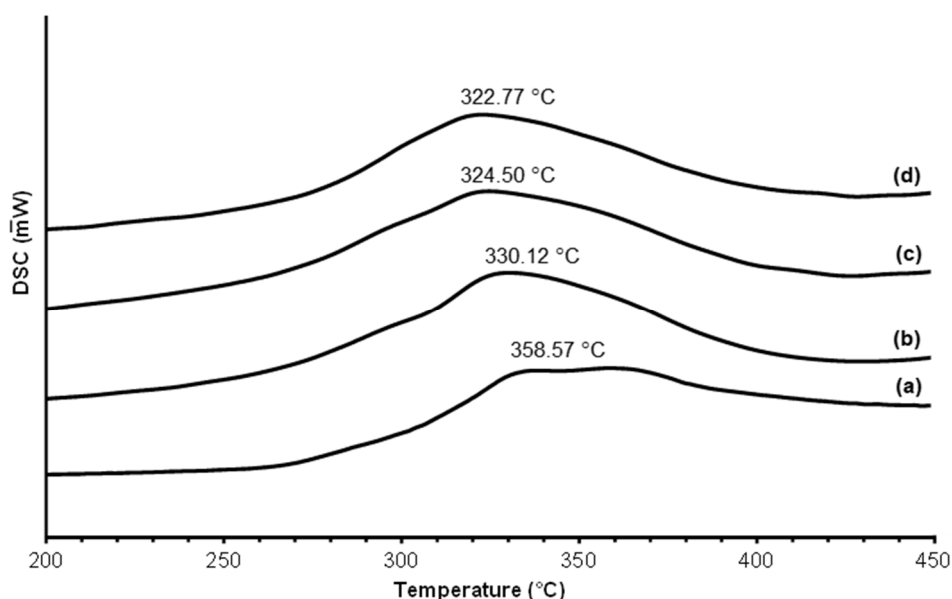


Fig 4. DSC spectra of BC irradiated with 0 (a), 25 (b), 50 (c), and 75 (d) kGy

Cytotoxicity Assay of Gamma-Irradiated BC

Cytotoxicity is an important characteristic of a material intended for biomedical applications. Cytotoxicity test of the gamma-irradiated BC was conducted using HeLa cells and the WST-8 assay, which is based on the conversion of a water-soluble tetrazolium salt to a water-soluble formazan dye upon reduction by dehydrogenases in the presence of an electron carrier [29].

The WST-8 assay of the adherent cell in the presence of the gamma-irradiated BC demonstrated low viability of the adherent cells after 24 h of incubation (Fig. 5). However, after 48 h of incubation, the adherent cells showed improved cell viability compared to those on day 1, indicating no cytotoxic effects of gamma-irradiated BC for cell proliferation. A previous report showed that the BC scaffold did not show any toxicity effect on BMSCs, while it increased cell viability [30].

Osteogenic Differentiation of rBMSCs on Gamma-Irradiated BC

To evaluate the potential of gamma-irradiated BC as a 3D scaffold for bone tissue regeneration, rBMSCs were seeded on BC scaffolds and incubated for 14 days in the presence of an osteogenic medium. The osteogenic differentiation of the rBMSCs was then evaluated by assessing calcium deposition on irradiated BC by ARS

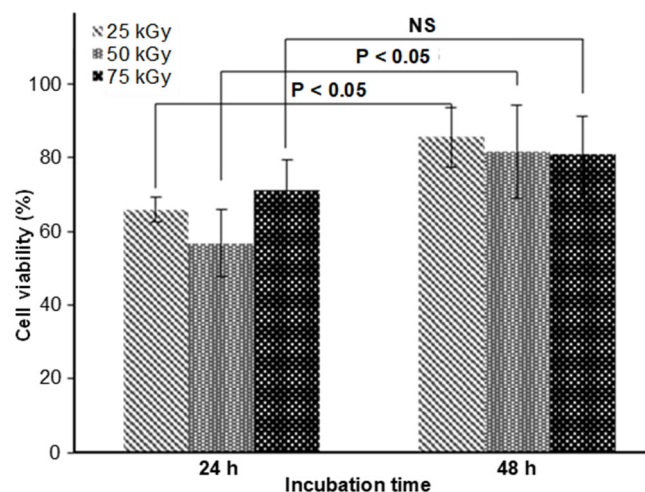


Fig 5. Cytotoxicity assay of gamma-irradiated BC against HeLa Cells. NS = not significant

staining. ARS compound reacts with calcium ions to form an ARS-calcium complex in a chelation process [30].

After 14 days of incubation, ARS staining revealed that BC scaffolds with higher irradiation doses showed intense staining indicating higher calcium deposition (Fig. 6). The difference in the ARS staining of the gamma-irradiated BC is probably due to the change of crystallinity of the BC caused by gamma irradiation, as confirmed by the XRD results. A previous report showed that the amorphous poly(caprolactone-co-glycolide) (PCL/PGA)

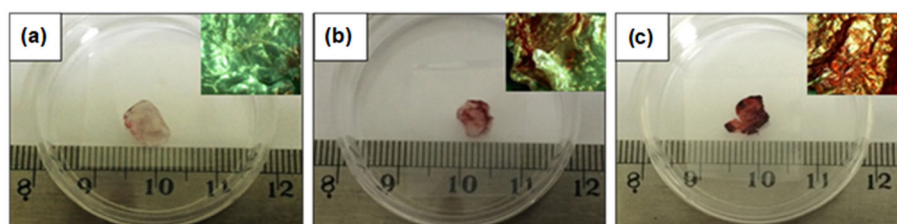


Fig 6. ARS staining of rBMSCs cultured on gamma-irradiated BC. BC pellicles exposed to 25 (a), 50 (b), or 75 (c) kGy of gamma irradiation were used

scaffold was significantly efficient in supporting osteoblast growth compared to highly crystalline and rigid PCL and PGA scaffolds [31]. However, it is not fully understood how crystallinity affects stem cell behavior [32]. Another possibility is from the increase of the carbonyl group in the gamma-irradiated BC, as confirmed by the FTIR measurement. The FTIR spectra showed that the intensities of the carbonyl peak of gamma-irradiated BC increased with increasing irradiation dose. It has already been known that functional groups of the scaffold may affect cell behaviors [33]. Carboxylic acid and carbonyl groups on the surface of PLGA/HA matrices containing graphene oxide improved bioactivity and osteogenic differentiation of MC3T3-E1 cells encapsulated in the matrices [34].

This study revealed that gamma-irradiated BC supported osteogenic differentiation of rBMSCs, as shown by ARS staining. However, the biodegradation properties and *in vitro* cell behavior inside the gamma-irradiated BC were not used in this study to investigate the basic characterization in terms of the application of gamma-irradiated BC as 3D scaffolds for tissue regeneration, which is the next step we need to investigate.

■ CONCLUSION

Our findings show that gamma-irradiation has a significant effect on the physical, chemical, and thermal properties of BC, as confirmed by FTIR, XRD, and DSC analyses. ARS staining demonstrated that rBMSCs seeded on gamma-irradiated BC and incubated in an osteogenic medium for 14 days produce calcium as a late marker for osteogenic differentiation. Higher irradiation doses of gamma-irradiated BC showed intense ARS staining, indicating higher calcium deposition. These findings show that gamma-irradiation can be used to create a

cytocompatible 3D scaffold for tissue engineering. An additional investigation should be conducted to further analyze interactions between cells and gamma-irradiated BC.

■ ACKNOWLEDGMENTS

This research was supported in part by the NAIST global collaboration project (FY2016-2018) funded by MEXT, Japan, and DIPA (2019) from the Center for Research of Radiation Processing Technology, National Nuclear Energy Agency. In addition, we thank Shohei Katao for his assistance in XRD measurements.

■ REFERENCES

- [1] Caliari, S.R., and Burdick, J.A., 2016, A practical guide to hydrogels for cell culture, *Nat. Methods*, 13 (5), 405–414.
- [2] Choe, G., Park, J., Park, H., and Lee, J.Y., 2018, Hydrogel biomaterials for stem cell microencapsulation, *Polymers*, 10 (9), 1–17.
- [3] Li, X., Sun, Q., Li, Q., Kawazoe, N., and Chen, G., 2018, Functional hydrogels with tunable structures and properties for tissue engineering applications, *Front. Chem.*, 6, 499.
- [4] Torgbo, S., and Sukyai, P., 2018, Bacterial cellulose-based scaffold materials for bone tissue engineering, *Appl. Mater. Today*, 11, 34–49.
- [5] Pang, M., Huang, Y., Meng, F., Zhuang, Y., Liu, H., Du, M., Ma, Q., Wang, Q., Chen, Z., Chen, L., Cai, T., and Cai, Y., 2020, Application of bacterial cellulose in skin and bone tissue engineering, *Eur. Polym. J.*, 122, 109365.
- [6] Hickey, R.J., and Pelling, A.E., 2019, Cellulose biomaterials for tissue engineering, *Front. Bioeng. Biotechnol.*, 7, 45.

- [7] Portela, R., Leal, C.R., Almeida, P.L., and Sobral, R.G., 2019, Bacterial cellulose: A versatile biopolymer for wound dressing applications, *Microb. Biotechnol.*, 12 (4), 586–610.
- [8] Cherng, J.H., Chou, S.C., Chen, C.L., Wang, Y.W., Chang, S.J., Fan, G.Y., Leung, F.S., and Meng, E., 2021, Bacterial cellulose as a potential bio-scaffold for effective re-epithelialization therapy, *Pharmaceutics*, 13 (10), 1592.
- [9] Criado, P., Frascini, C., Jamshidian, M., Salmieri, S., Safrany, A., and Lacroix, M., 2017, Gamma-irradiation of cellulose nanocrystals (CNCs): Investigation of physicochemical and antioxidant properties, *Cellulose*, 24 (5), 2111–2124.
- [10] Gorgieva, S., and Trček, J., 2019, Bacterial cellulose: Production, modification and perspectives in biomedical applications, *Nanomaterials*, 9 (10), 1352.
- [11] Unal, S., Arslan, S., Yilmaz, B.K., Oktar, F.N., Sengil, A.Z., and Gunduz, O., 2021, Production and characterization of bacterial cellulose scaffold and its modification with hyaluronic acid and gelatin for glioblastoma cell culture, *Cellulose*, 28 (1), 117–132.
- [12] Bayir, E., Bilgi, E., Hames, E.E., and Sendemir, A., 2019, Production of hydroxyapatite–bacterial cellulose composite scaffolds with enhanced pore diameters for bone tissue engineering applications, *Cellulose*, 26 (18), 9803–9817.
- [13] Popa, L., Ghica, M.V., Tudoroiu, E.E., Ionescu, D.G., and Dinu-Pîrvu, C.E., 2022, Bacterial cellulose–A remarkable polymer as a source for biomaterials tailoring, *Materials*, 15 (3), 1054.
- [14] Nurlidar, F., and Kobayashi, M., 2019, Succinylated bacterial cellulose induce carbonated hydroxyapatite eposition in a solution mimicking body fluid, *Indones. J. Chem.*, 19 (4), 858–864.
- [15] da Silva Aquino, K.A., 2012, "Sterilization by Gamma Irradiation" in *Gamma Radiation*, Eds. Adrovic, F., IntechOpen, Rijeka, Croatia.
- [16] Pérez Davila, S., González Rodríguez, L., Chiussi, S., Serra, J., and González, P., 2021, How to sterilize polylactic acid based medical devices?, *Polymers*, 13 (13), 2115.
- [17] Baccaro, S., Carewska, M., Casieri, C., Cemmi, A., and Lepore, A., 2013, Structure modifications and interaction with moisture in γ -irradiated pure cellulose by thermal analysis and infrared spectroscopy, *Polym. Degrad. Stab.*, 98 (10), 2005–2010.
- [18] Bouchard, J., Méthot, M., and Jordan, B., 2006, The effects of ionizing radiation on the cellulose of woodfree paper, *Cellulose*, 13 (5), 601–610.
- [19] Darwis, D., Khusniya, T., Hardiningsih, L., Nurlidar, F., and Winarno, H., 2012, In-vitro degradation behaviour of irradiated bacterial cellulose membrane, *Atom Indones.*, 38 (2), 78–82.
- [20] Ferro, M., Mannu, A., Panzeri, W., Theeuwens, C.H.J., and Mele, A., 2020, An integrated approach to optimizing cellulose mercerization, *Polymers*, 12 (7), 1559.
- [21] Wojdyr, M., 2010, Fityk: A general-purpose peak fitting program, *J. Appl. Crystallogr.*, 43 (5-1), 1126–1128.
- [22] Park, S., Baker, J.O., Himmel, M.E., Parilla, P.A., and Johnson, D.K., 2010, Cellulose crystallinity index: Measurement techniques and their impact on interpreting cellulase performance, *Biotechnol. Biofuels*, 3 (1), 10.
- [23] Wada, M., Sugiyama, J., and Okano, T., 1993, Native celluloses on the basis of two crystalline phase (I α /I β) system, *J. Appl. Polym. Sci.*, 49 (8), 1491–1496.
- [24] Ju, X., Bowden, M., Brown, E.E., and Zhang, X., 2015, An improved X-ray diffraction method for cellulose crystallinity measurement, *Carbohydr. Polym.*, 123, 476–481.
- [25] Luo, H., Li, W., Yang, Z., Ao, H., Xiong, G., Zhu, Y., Tu, J., and Wan, Y., 2018, Preparation of oriented bacterial cellulose nanofibers by flowing medium-assisted biosynthesis and influence of flowing velocity, *J. Polym. Eng.*, 38 (3), 299–305.
- [26] Eo, M.Y., Fan, H., Cho, Y.J., Kim, S.M., and Lee, S.K., 2016, Cellulose membrane as a biomaterial: From hydrolysis to depolymerization with electron beam, *Biomater. Res.*, 20 (1), 16.
- [27] Liu, Y., Chen, J., Wu, X., Wang, K., Su, X., Chen, L., Zhou, H., and Xiong, X., 2015, Insights into the effects of γ -irradiation on the microstructure, thermal stability and irradiation-derived

- degradation components of microcrystalline cellulose (MCC), *RSC Adv.*, 5 (43), 34353–34363.
- [28] Soares, S., Camino, G., and Levchik, S., 1995, Comparative study of the thermal decomposition of pure cellulose and pulp paper, *Polym. Degrad. Stab.*, 49 (2), 275–283.
- [29] Chamchoy, K., Pakotiprapha, D., Pumirat, P., Leartsakulpanich, U., and Boonyuen, U., 2019, Application of WST-8 based colorimetric NAD(P)H detection for quantitative dehydrogenase assays, *BMC Biochem.*, 20 (1), 4.
- [30] Vadaye Kheiry, E., Parivar, K., Baharara, J., Fazly Bazzaz, B.S., and Iranbakhsh, A., 2018, The osteogenesis of bacterial cellulose scaffold loaded with fisetin, *Iran. J. Basic Med. Sci.*, 21 (9), 965–971.
- [31] Cui, H., and Sinko, P.J., 2012, The role of crystallinity on differential attachment/proliferation of osteoblasts and fibroblasts on poly (caprolactone-co-glycolide) polymeric surfaces, *Front. Mater. Sci.*, 6 (1), 47–59.
- [32] Kaivosoja, E., Barreto, G., Levón, K., Virtanen, S., Ainola, M., and Konttinen, Y.T., 2012, Chemical and physical properties of regenerative medicine materials controlling stem cell fate, *Ann. Med.*, 44 (7), 635–650.
- [33] Klecker, C., and Nair, L.S., 2017, "Matrix Chemistry Controlling Stem Cell Behavior" in *Biology and Engineering of Stem Cell Niches*, Eds. Vishwakarma, A., and Karp, J.M., Academic Press, Boston, US, 195–213.
- [34] Fu, C., Bai, H., Zhu, J., Niu, Z., Wang, Y., Li, J., Yang, X., and Bai, Y., 2017, Enhanced cell proliferation and osteogenic differentiation in electrospun PLGA/hydroxyapatite nanofibre scaffolds incorporated with graphene oxide, *PLoS One*, 12 (11), e0188352.